Measurement of Lateral Charge Propagation in $[Os(bpy)_2(PVP)_nCl]Cl$ Thin Films: A Scanning Electrochemical Microscopy Approach

A. P. O'Mullane, J. V. Macpherson, and P. R. Unwin*

Department of Chemistry, University of Warwick, Coventry CV4 7AL, U.K.

J. Cervera-Montesinos and J. A. Manzanares

Department of Thermodynamics, Faculty of Physics, University of Valencia, E-46100 Burjasot, Spain

F. Frehill and J. G. Vos

School of Chemical Sciences, Dublin City University, Dublin 9, Ireland

Received: February 4, 2004; In Final Form: March 24, 2004

The use of scanning electrochemical microscopy (SECM) to measure charge transport diffusion constants (D_{CT}) in metallopolymers of the type $[Os(bpy)_2(PVP)_nCl]Cl$, bpy = 2,2′-bipyridyl and PVP = poly(4-vinylpyridine), is described. In this approach, a triple potential step technique is employed in which the ultramicroelectrode (UME) tip of the SECM is used to electrogenerate a solution phase oxidant, $Ru(CN)_6^{3-}$, in an initial potential step, via the oxidation of $Ru(CN)_6^{4-}$. This moiety diffuses from the tip to the underlying polymer film where electron transfer occurs, causing the local oxidation of the polymer-bound complex of Os^{II} to Os^{III}. The form of the current−time characteristic in this step provides information on the kinetics of the ET process between the solution species and the polymer-bound moiety, as well as the concentration of redox-active species in the polymer film. This process creates lateral concentration gradients of Os^{II} and Os^{III} along the film. After the first potential step, a waiting period is introduced in which $Ru(CN)_6^{3-}$ is converted back to $Ru(CN)_6^{4-}$ at the UME and Os^{II} can recover in concentration by electron self-exchange between Os^{III} and Os^{II} moieties. After a defined time, the potential of the UME is switched again to cause the generation of the solution-phase oxidant, $Ru(CN)_6^{3-}$. The current−time behavior associated with this step is influenced significantly by the extent of lateral electron hopping in the waiting period. It is shown that SECM is capable of measuring D_{CT} values as low as 10^{-10} cm^2 s^{-1} with good precision. We report experimental measurements on spin-coated films of $[Os(bpy)_2(PVP)_nCl]Cl$, where n = 5 or 10, which indicate that D_{CT} is affected significantly by redox site loading and film structure (as determined by atomic force microscopy).

Introduction

Metallopolymers of the type $[M(bpy)_2(Pol)_nCl]Cl$, where M = Ru or Os, bpy = 2,2′-bipyridyl and Pol = poly(4-vinyl-4-vinylpyridine) (PVP), or poly(*N*-vinylimidazole) (PVI), have received much attention.[1−11] This is due to their potential widespread applications in areas such as sensors, electronic devices, energy storage, and corrosion protection.[10] A possible future application is in the area of molecular electronics where this class of material may act as a linker between metallic nanoparticles, which could be electrochemically switched.

Electron and charge transfer through thin films of metallopolymers on electrode surfaces has been studied extensively.[12−27] It is widely accepted that charge propagation through redox polymers is limited by one of three processes: (i) electron-self-exchange between redox moieties in the film, (ii) the rate of ion diffusion into or out of the film to maintain electroneutrality, and (iii) the degree of polymer chain rearrangement required to juxtapose redox centers. Conventional techniques employed to study charge transport in redox polymers include cyclic voltammetry (CV), potential step chronoamperometry (CA),[3−8] and to a lesser extent, electrochemical impedance spectroscopy (EIS).[28−30] However, there is often a discrepancy in the charge transport coefficients (normally denoted D_{CT}) determined by CV (usually of the order 10^{-10} cm^2 s^{-1}) and CA; the latter measurements often yield D_{CT} values that are an order of magnitude higher than from CV.

It has been suggested that D_{CT} determined by potential step methods is often limited by ion diffusion into the film,[3] whereas for voltammetry the limitation is either polymer chain movement at low redox center loadings/high electrolyte concentration combinations, or ion diffusion at high redox center loadings. Yet, when ion diffusion is regarded as the limiting process, there is still a discrepancy between CV and CA, presumably because the extent of ion movement is distinctively different in these techniques. In CV, over 80% of redox sites in the film are typically oxidized,[3] resulting in widespread ion diffusion within the film and ingress/egress at the film−electrolyte interface. In contrast, the potential step experiments are often made on a shorter time scale, so that ion diffusion within the film is less extensive and probably involves counterions already present in the film. For EIS, the system is perturbed only slightly from the steady state, so that a small fraction of redox states in the film is active during the measurement, most probably charge-compensated by counterions that are already within the film. D_{CT} values on the order of 10^{-8} cm^2 s^{-1} have been reported for $[Os(bpy)_2(PVP)_nCl]Cl$,[29] using this latter technique, which is within the range obtained from steady-state techniques, where ion diffusion and polymer chain movement are no longer

10.1021/jp049500v CCC: $27.50
Published on Web 05/05/2004

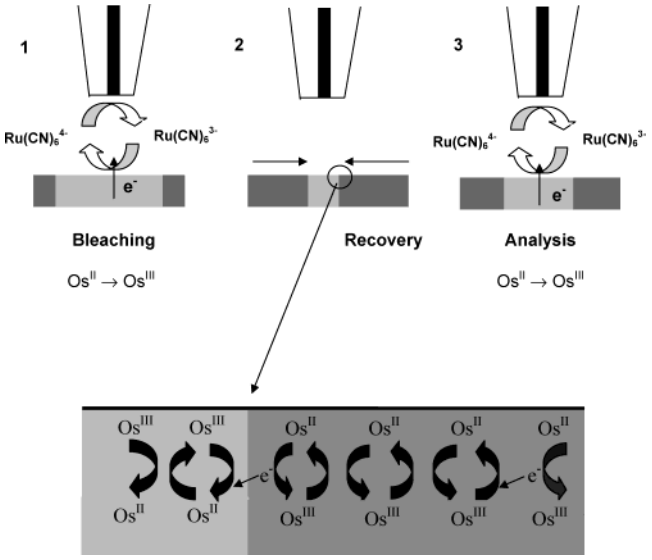

Figure 1. Schematic of the triple step transient technique for measuring lateral charge propagation.

limiting factors.[14,31,32] For (Os II/III) electropolymerized systems, values as high as 10^{-6} cm^2 s^{-1} have been reported for D_{CT}[14] under steady-state conditions.

In this work we investigate the rate of lateral charge propagation in relatively thin films of $[Os(bpy)_2(PVP)_nCl]Cl$ and describe how scanning electrochemical microscopy (SECM) may be used to determine D_{CT}. Several methods have previously been employed to measure lateral charge propagation in thin film and monolayer systems. Majda and co-workers[33,34] have used two-dimensional voltammetric measurements carried out with line microelectrodes to study lateral charge transport in Langmuir monolayers. Murray's group[35,36] used generation-collection measurements at microband electrode arrays to measure lateral charge propagation in polymer films, under both steady-state and time-dependent conditions. Forster and co-workers have used ultramicroelectrodes (UMEs) to measure charge transport dynamics of solid-state osmium bis(bipyridyl)-tetrazine chloride films.[37]

The experimental method employed in this paper utilizes transient SECM measurements. Following initial work on lateral proton transfer in this laboratory,[38−40] SECM has recently been used to study charge injection and lateral propagation in Langmuir−Blodgett films of polyaniline (PANI),[41] the conductivity of PANI monolayers[42] and the lateral (physical) diffusion of *N*-octadecylferrocenecarboxamide ($C_{18}Fc$) in a Langmuir monolayer.[43] Other groups have also recognized the possibility of using SECM to measure lateral charge transport and conductivity in monolayer systems.[44,45]

To study the lateral diffusion of the amphiphile, $C_{18}Fc$, in a mixed Langmuir monolayer, a triple potential step experiment was devised[43] analogous to fluorescence recovery after photobleaching (FRAP), which is widely used to measure lateral diffusion in biomembranes.[46−49] Here, we show how this SECM triple potential step method may be used to measure diffusion constants for charge propagation in a thin film of a redox polymer, illustrated by studies of the $[Os(bpy)_2(PVP)_nCl]Cl$ system. The basic idea is illustrated schematically in Figure 1. An UME is positioned close to the interface between the polymer film and solution and used to electrogenerate a redox species in solution (oxidation of $Ru(CN)_6^{4-}$ to $Ru(CN)_6^{3-}$; step 1). This species diffuses from the UME to the polymer film where electron transfer occurs locally (eq 1).

$$Os^{II}_{film} + Ru(CN)_6^{3-}{}_{aq} \leftrightarrow Os^{III}_{film} + Ru(CN)_6^{4-}{}_{aq} \quad (1)$$

The kinetics and extent of this process controls the diffusion of the solution product of the reaction, $Ru(CN)_6^{4-}$, back to the UME.

As discussed fully in our previous paper,[43] one can measure the ET kinetics and determine the concentration of redox moieties at the target interface from the current−time response recorded at the UME in this step. For the case of low D_{CT}, the electrode induced process is largely confined to the portion of the film directly under the tip of the UME.[43] Next, there is a waiting period (step 2), in which $Ru(CN)_6^{3-}$ quickly recovers to $Ru(CN)_6^{4-}$ in the gap between the UME and film surface. On a much longer time scale, lateral charge propagation within the polymer film may occur, for example, by electron hopping. For the system here, this process involves electron self-exchange between Os^{II} and Os^{III} moieties that have a lateral gradient in the film, due to the local redox process in step 1. Finally, step 3 is a repeat of step 1, involving oxidant electrogeneration at the tip. The form of the current−time transient for this step may contain information on charge propagation in the film (during the recovery period), depending on the time scale of step 2 relative to D_{CT}. If step 2 is very short (compared to the lateral charge-transfer diffusion time), and the film is extensively oxidized in step 1, the third step shows a current−time response similar to an inert surface. In this case, one can determine the tip−interface separation from the chronoamperometric curve.[43] On the other hand, if the second step is sufficiently long, D_{CT} can be determined from the current−time response in step 3, as there will be a repopulation of Os^{II} moieties, by lateral charge propagation into the zone of the film probed by the UME. This serves to enhance the current response for the third (analysis) step, as it provides reagent in the film for reaction with electrogenerated oxidant.

In earlier work,[43] we studied the physical diffusion of a surfactant with a relatively high lateral diffusion coefficient (ca. 10^{-6} cm^2 s^{-1}). Here, we show that SECM is capable of measuring much lower D_{CT}, as found in redox polymer systems. An advantage of SECM is that the film of interest need not be deposited on an electrode, as charge injection occurs from a solution redox species, which can be tuned to give optimal conditions for the redox reaction. Furthermore, in contrast to conventional time-dependent techniques, the redox reaction and accompanying charge compensation process occur from the same side of the film (starting at the film/electrolyte interface and proceeding across to the underlying inert solid on which the film is deposited). This may be more efficient than CV or CA studies of films on electrodes, where the redox process starts with heterogeneous electron transfer at the electrode/film boundary and charge compensation establishes an ion flux at the film/electrolyte interface, on the opposite side of the film.

Theory

We have treated the triple potential step problem previously, for the case of lateral diffusion in a monolayer.[43] The time scales were relatively short, so that we did not have to be concerned with the spatial domain beyond the thin gap between the tip and interface of interest, allowing us to fix the concentrations at the edge of this zone to the bulk values. In the present study, where much longer time scales are involved, we have avoided setting the conditions in this way. Although there are similarities in the two models, we outline the problem here, as it pertains to the redox polymer system, because this provides a context for results from the model which are reported later.

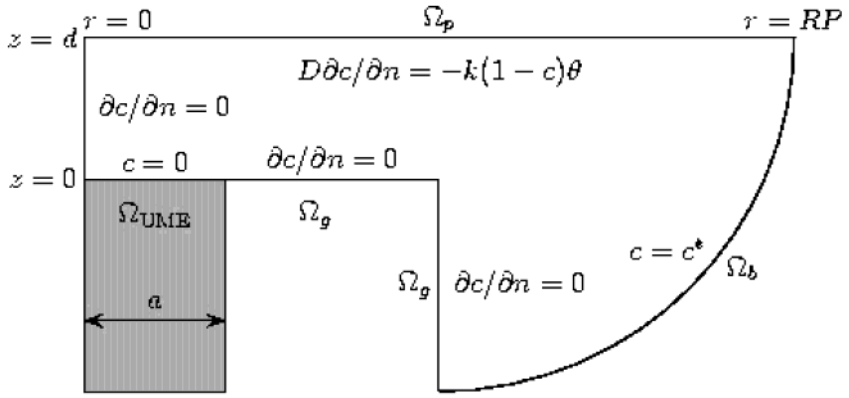

Figure 2. Schematic view (not to scale) of the domain used for the numerical calculations. The boundary conditions imposed to the transport equation of $Ru(CN)_6^{4-}$ are shown. The surface Ω_g is defined as $(z - d)^2 + (r - 10a)^2 = (RP - 10a)^2$, $z \le d$, $r \ge 10a$.

The coordinate system and principal boundary conditions pertaining to the first potential step in the experiment of interest are depicted in Figure 2.

The presence of an excess supporting electrolyte allows us to describe the transport of $Ru(CN)_6^{4-}$, which is in bulk solution at concentration, c^*, as a diffusional process:

$$\frac{\partial c}{\partial t} = D\left(\frac{\partial^2 c}{\partial r^2} + \frac{1}{r}\frac{\partial c}{\partial r} + \frac{\partial^2 c}{\partial z^2}\right) \tag{2}$$

where c and D are the concentration and diffusion coefficient of $Ru(CN)_6^{4-}$, r and z are the radial and axial coordinates (see Figure 2) and t is time. Initially, the concentration of $Ru(CN)_6^{4-}$ is that of the bulk

$$c(r,z) = c^* \qquad t = 0 \tag{3}$$

In the first step (period $t < \Delta t_1$) we apply a sufficiently driving potential to the UME so that $Ru(CN)_6^{4-}$ is oxidized to $Ru(CN)_6^{3-}$ under diffusion control. The boundary condition at the UME, delimited by surface Ω_{UME}, is then

$$c = 0 \qquad \text{at } \Omega_{UME} \qquad 0 < t < \Delta t_1 \tag{4}$$

The electrogenerated $Ru(CN)_6^{3-}$ ions diffuse away from the UME and reach the polymer film, where they are reduced back to $Ru(CN)_6^{4-}$ by oxidizing the polymer (eq 1). In this process, the polymer acts as a sink for the flux of $Ru(CN)_6^{4-}$. The flux density of $Ru(CN)_6^{3-}$ at the polymer/electrolyte interface Ω_p is controlled by the boundary condition

$$D'\left.\frac{\partial c'}{\partial z}\right|_{z=d} = kc'\theta \tag{5}$$

where D' and c' are the diffusion coefficient and concentration of $Ru(CN)_6^{3-}$, respectively, k is the rate constant for the polymer oxidation, $\theta(r,t)$ is the local fraction of the polymer in the reduced state, and Ω_p is the polymer surface. The time variation of $\theta(r,t)$ depends on the oxidation rate induced by the flux of $Ru(CN)_6^{3-}$ and the recovery process of the polymer. It is described by

$$\frac{\partial \theta}{\partial t} = -\frac{kc'\theta}{\Gamma} + D_{CT}\left(\frac{\partial^2 \theta}{\partial r^2} + \frac{1}{r}\frac{\partial \theta}{\partial r}\right) \tag{6}$$

where Γ (mol cm^{-2}) is the effective surface concentration of osmium redox centers in the thin polymer film. Note that this formulation assumes that there are no diffusional limitations across the thickness of the film (from the electrolyte/film boundary to the underlying film/substrate boundary), only in the radial direction. This is reasonable, in light of the experimental results that follow, compounded by the fact that the film thickness ($l_{film} \sim 100$ nm), is much less than the lateral dimension of the experiment, e.g., electrode radius, $a = 12.5$ μm; overall probe radius of 125 μm. The recovery process is assumed to be described by a diffusion-type equation for the lateral electron transport in the polymer. The initial and boundary conditions for eq 6 are

$$\theta(r) = 1 \qquad t = 0 \tag{7}$$

$$\frac{\partial \theta}{\partial r} = 0 \qquad r = 0 \tag{8}$$

$$\theta = 1 \qquad r = RP \tag{9}$$

Due to the continuity of mass, the flux density of $Ru(CN)_6^{3-}$ that is reduced at the polymer must be equal to the flux density of $Ru(CN)_6^{4-}$ that diffuses normal to the film

$$D\left.\frac{\partial c}{\partial z}\right|_{z=d} = -D'\left.\frac{\partial c'}{\partial z}\right|_{z=d} \tag{10}$$

We assume that the diffusion coefficients of $Ru(CN)_6^{3-}$ and $Ru(CN)_6^{4-}$ are equal, and because the total concentration in the system does not change, the local mass conservation is satisfied

$$c'(r,z) + c(r,z) = c^* \tag{11}$$

This allows c' to be replaced by by $c^* - c$ in eqs 5 and 6, so avoiding the need to solve an equation equivalent to eq 2 for c'. The rest of the boundary conditions of eq 2 are the symmetry condition,

$$\frac{\partial c}{\partial r} = 0 \qquad r = 0 \qquad 0 \le z \le d \tag{12}$$

the null flux density at the surface Ω_g of the glass sheath that covers the UME, which is inert to the species in solution,

$$D\frac{\partial c}{\partial z} = 0 \tag{13}$$

where Ω_g is the glass sheath surface, and the assumption that the concentration of $Ru(CN)_6^{4-}$ at the outer boundary of the system delimited by surface Ω_b is the bulk concentration during the whole experiment

$$c = c^* \qquad \text{at } \Omega_b \tag{14}$$

In the waiting period (step 2), the UME is held at a potential to quickly regenerate $Ru(CN)_6^{4-}$ from any $Ru(CN)_6^{3-}$ in its vicinity. Sufficient time elapses for the region of the polymer locally oxidized to recover by lateral electron transfer within the film, which involves the reduction of Os^{III} to Os^{II} in the film region in front of the UME and the oxidation of Os^{II} to Os^{III} in the outer film surface.

$$c = c^* \qquad \text{at } \Omega_{UME} \qquad \Delta t_1 < t < \Delta t_2 \tag{15}$$

The recovery process of the polymer is quite slow, and to have a substantial recovery, Δt_2 is of the order of tens to hundreds of minutes. For this reason the simulation domain was extended significantly with respect to prior studies using the three-step method.[43] The domain must be large enough so that $\theta = 1$ at r = RP and no $Ru(CN)_6^{3-}$ reaches Ω_b. Typically, RP = 40a, which marked one end of the quarter-circle boundary, Ω_b (Figure 2). The electrode probe had a glass insulator dimension 10 times that of the electrode itself, a.

In step 3, the potential at the UME was applied again to oxidize $Ru(CN)_6^{4-}$ to $Ru(CN)_6^{3-}$. The boundary conditions are those defined for step 1, but the length of step Δt_3 may be different from that of step 1. To proceed to the numerical integration of the differential equations, it is advisable to cast the problem into dimensionless form. We define the variables

$$\tau \equiv tD/a^2 \tag{16}$$

$$R \equiv r/a \tag{17}$$

$$Z \equiv z/a \tag{18}$$

$$C \equiv c/c^* \tag{19}$$

$$K \equiv ka/D \tag{20}$$

$$\gamma \equiv \Gamma/(ac^*) \tag{21}$$

$$D_r \equiv D_{CT}/D \tag{22}$$

The main equations of the problem in normalized form are

$$\frac{\partial C}{\partial \tau} = \frac{\partial^2 C}{\partial R^2} + \frac{1}{R}\frac{\partial C}{\partial R} + \frac{\partial^2 C}{\partial Z^2} \tag{23}$$

$$\frac{\partial \theta}{\partial \tau} = -\frac{K(1-C)\theta}{\gamma} + D_r\left(\frac{\partial^2 \theta}{\partial R^2} + \frac{1}{R}\frac{\partial \theta}{\partial R}\right) \tag{24}$$

$$\frac{\partial C}{\partial Z} = -K(1-C)\theta \qquad \text{at } Z = d/a \tag{25}$$

The problem was solved using the finite element method for the spatial dependency and the finite difference method for the time dependency. It was implemented using the commercial package Femlab. To compare the theoretical simulation with the experimental curves, the current−time response for the first and third steps is calculated from[50,51]

$$\frac{i}{i_\infty} = \frac{\pi}{2}\int_0^1 \left.\frac{\partial C}{\partial Z}\right|_{Z=0} R\, dR \tag{26}$$

where i_∞ is simply the steady-state current at an inlaid disk electrode:[52,53]

$$i_\infty = 4nFDac^* \tag{27}$$

where n is the number of electrons transferred ($n = 1$ in our case) and F is the Faraday constant.

There are four (normalized) parameters that influence the normalized current−time characteristic: d/a, K, γ, and D_r. In the three-step method, the distance is usually obtained by applying relatively long and short time intervals for steps 1 and 2, respectively, so that the redox moieties in the zone of the film probed by the UME essentially react to completion (in step 1) but there is insufficient time for any recovery process in step 2. In step 3, the polymer film then behaves as an inert substrate and the current depends only on d/a (because D is known). By applying the SECM theory in the inert substrate case, the distance between the UME and the polymer can be obtained.[43] However, in the experiments here, we also show that the redox reaction between $Ru(CN)_6^{3-}$ and the Os^{II} moiety in the film is characterized by a high value of K (diffusion-limited) so that initially in step 1, the probe current characteristics display pure positive feedback. This allows d in this interval within step 1 to be obtained. As the polymer is oxidized, its behavior departs from that of a pure conducting substrate, which allows us to fit γ. Finally, the fourth parameter, D_r, is obtained by letting the polymer partially recover in step 2, so that D_r is the only variable needed to fit the transient curve of step 3.

Experimental Section

Materials and Chemicals. $Os(bpy)_2(PVP)_nCl]Cl$ was prepared and characterized as described previously.[54,55] All chemicals were used as received and were $LiClO_4$ (Aldrich), potassium hexacyanoruthenate(II) hydrate (Strem chemicals), methanol (HPLC grade, Fisher chemicals), high purity acetone (Fisher chemicals), and propan-2-ol (HPLC grade, Fisher chemicals). All aqueous solutions were prepared from Milli-Q reagent water (Millipore Corp.).

Procedures. Glass and ITO substrates were cleaned by sonicating for 10 min in acetone and then in propan-2-ol and finally blown dry with nitrogen. Thin films of $[Os(bpy)_2(PVP)_nCl]Cl$ were spin coated (2500 rpm for 60 s) onto substrates by using a 1 wt % solution of the polymer in methanol. The thickness and topography of films were determined using both contact mode AFM (Digital Instruments, Nanoscope E) and tapping mode AFM (Digital Instruments, Multimode). Mean values of 90 ± 10 nm for $[Os(bpy)_2(PVP)_5Cl]Cl$ films and 100 ± 25 nm for $[Os(bpy)_2(PVP)_{10}Cl]Cl$ films were obtained.

CV measurements were made using a three-electrode arrangement. An ITO covered substrate, with a surface area of 0.35 cm^2, was used as the working electrode, a platinum gauze served as the counter electrode and a saturated calomel electrode (SCE) was used as the reference electrode. The SECM was a simple home-built instrument comprising a manual x, y, z stage (M-431, Newport Corp., CA) and a z-axis piezoelectric positioner and controller (models P-843.30 and E-501.00, Physik Instrumente, Waldbronn, Germany) to give fine control of the Pt UME working electrode in the direction normal to the sample. Transient SECM measurements of films on glass were carried out using a two electrode arrangement,[43] with a Pt UME as the working electrode and a silver wire as a quasi-reference electrode (AgQRE). Transients were recorded with the probe UME positioned at fresh spots on the sample, with a separation of at least 200 μm from the regions of any previous measurements. The Pt UME used was a 25 μm diameter disk electrode with a glass insulating sheath, characterized by an RG value of 10 ($RG = r_{glass}/a$; where r_{glass} is the radius of the sheath around the probe). Cyclic voltammetry and current−time transients were recorded using an electrochemical analyzer (CH Instruments,

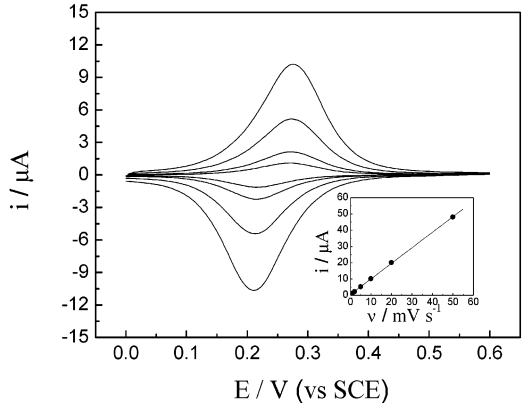

Figure 3. Cyclic voltammograms for an ITO electrode covered with $[Os(bpy)_2(PVP)_5Cl]Cl$ in 0.1 M $LiClO_4$ at 1, 2, 5, and 10 mV s^{-1}. The inset shows the linear relationship between anodic peak current and sweep rate.

model CHI730A). The diffusion coefficient of $Ru(CN)_6^{4-}$ was deduced by steady-state microdisk measurements in a bulk solution of 0.1 M $LiClO_4$ and 0.2 mM $Ru(CN)_6^{4-}$ yielding a value of $(7.46 \pm 0.03) \times 10^{-6}$ cm^2 s^{-1}. This solution was used for all SECM measurements reported.

Results and Discussion

Voltammetry of Spin Cast Films. Although there are several reports on the electrochemistry of film electrodes of the type of interest here,[3,4,7,9,10,54] these previous studies are generally for much thicker drop cast films where values obtained for D_{CT} for $[Os(bpy)_2(PVP)_5Cl]Cl$ are of the order of[3] 1.3×10^{-11} cm^2 s^{-1}. In this work, we use much thinner spin cast films. Typical slow sweep cyclic voltammograms for an $[Os(bpy)_2(PVP)_5Cl]Cl$ spin cast film in 0.1 M $LiClO_4$ electrolyte are shown in Figure 3. There is a linear relationship between the peak current and sweep rate, when the latter is less than 100 mV s^{-1}, as illustrated by the inset of Figure 3. The peak to peak separation (ΔE_p) is 60 mV, and the full width at half-maximum current (fwhm) is 120 mV. This latter value is broader than expected for an ideal single electron process (90.6 mV) and may be due to repulsive interactions between redox centers[5] or heterogeneity in the film. The surface coverage of osmium redox centers in the films was determined from slow sweep cyclic voltammetry (1 mV s^{-1}) in 0.1 M $LiClO_4$, by integrating the charge under the oxidation and reduction peaks [$(4.6 \pm 0.6) \times 10^{-9}$ mol cm^{-2}].

SECM Measurements. To measure the electron-transfer kinetics between the Os^{II} redox centers in a $[Os(bpy)_2(PVP)_5Cl]$-Cl film and the solution mediator, SECM CA experiments were undertaken with the tip in close proximity to the film, deposited on an inert glass substrate. These measurements involved stepping the tip potential from 0 V (vs SCE) where no faradaic process occurred to 1.0 V, where the oxidation of $Ru(CN)_6^{4-}$ occurred at a diffusion-controlled rate. Figure 4 illustrates the current−time responses recorded at several different distances varying from 1.7 to 11 μm above the $[Os(bpy)_2(PVP)_5Cl]Cl$ film. The tip currents, i, have been normalized by the steady-state diffusion-limited current, i_∞, recorded in bulk solution. Values for each of the distances were obtained from the long time current response, when Os^{II} is effectively depleted at the portion of the film under the electrode.

The form of the current transient responses is as follows: after an initial charging current the faradaic current quickly decays to a quasi steady-state value, due to the feedback process illustrated in Figure 1, which subsequently falls to a hindered

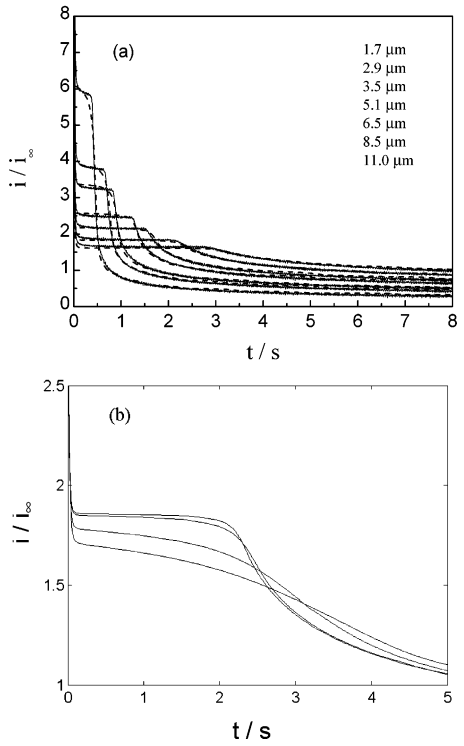

Figure 4. (a) Current−time responses of a Pt UME held at different distances, from 1.7 (top curve) to 11 μm (bottom curve) above a $[Os(bpy)_2(PVP)_5Cl]Cl$ spin cast film. The UME potential was stepped from 0 to 1.0 V (vs SCE) in a 0.2 mM $Ru(CN)_6^{4-}$ and 0.1 M $LiClO_4$ solution to generate $Ru(CN)_6^{3-}$ at a diffusion-limited rate. The thick lines are the experimental results and the dashed lines are the modeled results (see text). (b) Simulated results, showing the effect of k on the current−time response recorded for step 1. Values of k (bottom to top) = 0.05, 0.1, 0.5, and 1 cm s^{-1}, $d = 8.5$ μm, $D_{CT} = 0$, and $\Gamma = 3.5 \times 10^{-9}$ mol cm^{-2} were employed.

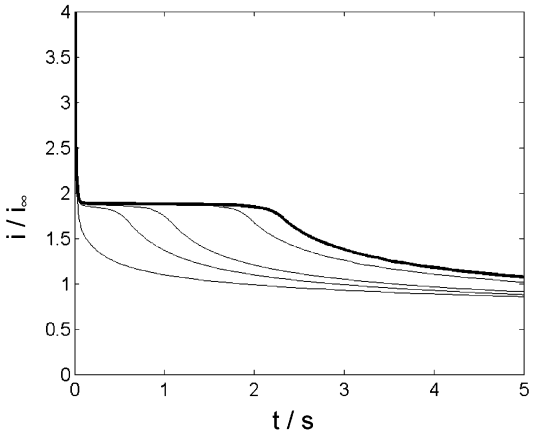

Figure 5. Simulated results showing the effect of D_{CT} on the current−time response for step 3 with the periods for step 1 (5 s) and 2 (waiting time of 30 min) kept constant. D_{CT} was varied as follows: 7.5×10^{-11} (fine curve on left), 3.8×10^{-10}, 7.5×10^{-10}, and 3.8×10^{-9} (fine curve on right) cm^2 s^{-1}. The thick line (on the right) is the transient for step 1. The following parameters were used: $d = 8.5$ μm, $D_{CT} = 0$, $\Gamma = 3.5 \times 10^{-9}$ mol cm^{-2}, $k = 1$ cm s^{-1}.

diffusion-limited value. The SECM current response also shows a strong distance effect; the closer the tip/surface distance, the larger is the initial feedback response and the earlier the subsequent fall in current. This can be explained as follows: $Ru(CN)_6^{3-}$ generated at the UME diffuses and reacts with the Os^{II} centers within the film until the whole area of the film opposite the electrode is oxidized. On the time scale of this

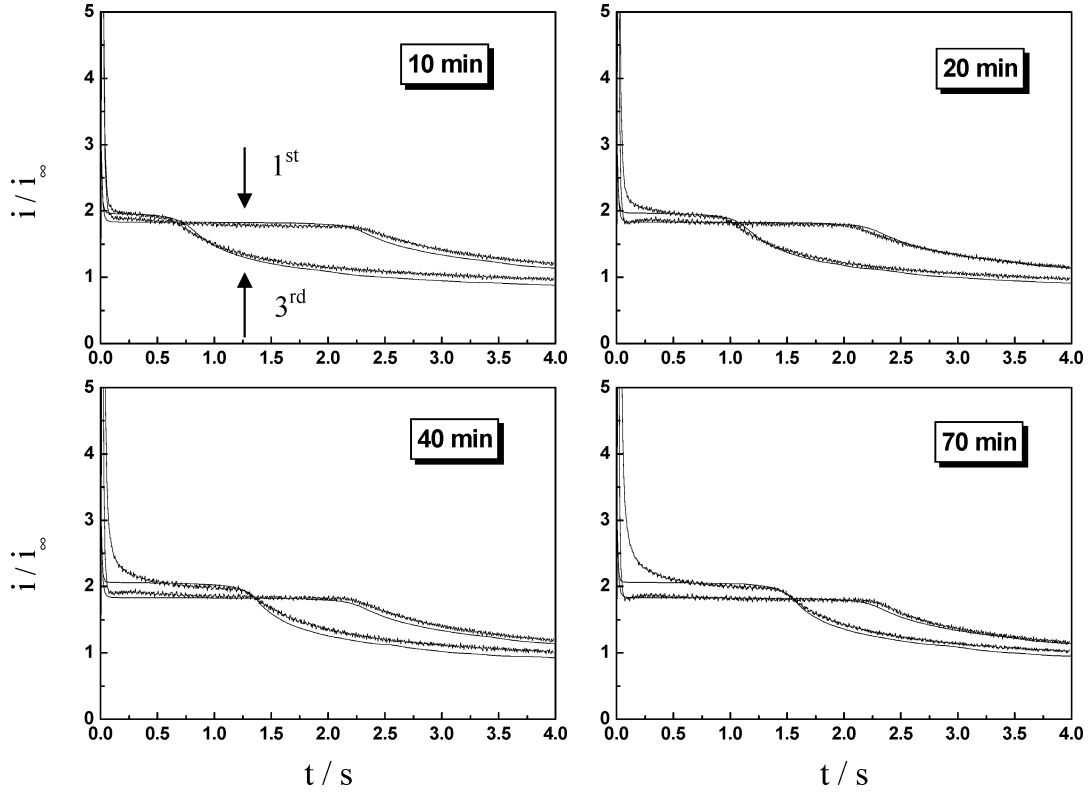

Figure 6. Current−time transients (for the first and third steps) to show the effect of waiting time (see box in each plot) on the recovery of charge carriers in a $[Os(bpy)_2(PVP)_5Cl]Cl$ film. The thick lines are the experimental results, and the thin lines are the modeled results using a value of 1.9×10^{-9} cm^2 s^{-1} for D_{CT}. For step 1: $d = 8.5$ μm, $D_{CT} = 0$, $\Gamma = 3.5 \times 10^{-9}$ mol cm^{-2}, $k = 1$ cm s^{-1}. For step 3 the same parameters were used, except $d = 7.5$ μm (10 and 20 min waiting time) and $d = 7$ μm (40 and 70 min waiting time).

first step there is effectively no lateral charge propagation within the film to regenerate the Os^{II} centers (because D_{CT} is comparatively small) and so the current falls. With an increase in the flux of $Ru(CN)_6^{4-}$ from the tip, due to feedback, as the distance between the tip and the surface decreases, this electrochemical "bleaching" process occurs faster and so results in an earlier fall in the probe current.

Figure 4 also shows the simulated current−time transients, which are seen to match extremely well with experiment. As discussed in the Theory, the parameters involved in this step are the concentration of redox centers in the film, the concentration and diffusion coefficient of the solution mediator, $Ru(CN)_6^{4-}$, the tip−sample distance, electron-transfer kinetics between the solution mediator and the polymer redox centers, and D_{CT}, which is taken as zero on this time scale. Having obtained d as described above, k was deduced from the initial plateau current of each transient. The best fit was obtained for diffusion-limited electron transfer between $Ru(CN)_6^{3-}$ and the Os^{II} redox centers ($k \geq 1$ cm s^{-1}). A rapid reaction is not unexpected for this outer sphere electron-transfer process for which the driving force is large, as judged by the fact that the oxidation wave observed in Figure 3 occurs at ca. 0.27 V (SCE) compared to the formal potential of the $Ru(CN)_6^{4-/3-}$ couple of 0.68 V (vs SCE).

The influence of k on the response for this first step is illustrated in Figure 4b, through simulations for a typical case of a tip−substrate distance of 8.5 μm, $D_{CT} = 0$, and $\Gamma = 3.5 \times 10^{-9}$ mol cm^{-2} and by using a redox mediator concentration ($Ru(CN)_6^{4-}$) of 0.2 mM that has a diffusion coefficient of 7.46×10^{-6} cm^2 s^{-1}. It can clearly be seen that the initial response converges to a limit at $k = 1$ cm s^{-1}, where the reaction is effectively controlled by feedback diffusion between the tip and the surface. Once k was known, the charge carrier concentration could be determined by varying this parameter to obtain the best fit to the decay of the transient between the positive feedback and hindered diffusion regimes. $\Gamma = (3.5 \pm 0.2) \times 10^{-9}$ mol cm^{-2} gave the best fit to the transients at all tip-interface distances. This corresponds reasonably well with the coverage of $(4.6 \pm 0.6) \times 10^{-9}$ mol cm^{-2} obtained from the CV measurements.

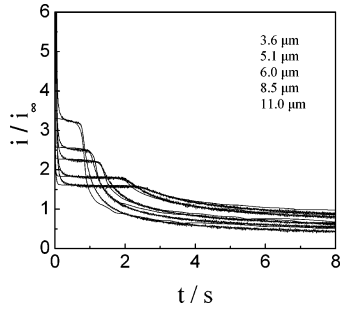

Figure 7. Current−time response (first potential step) of a Pt UME held at different distances, from 3.6 (top curve) to 11 (bottom curve) μm above a $[Os(bpy)_2(PVP)_{10}Cl]Cl$ spin cast film. The UME potential was stepped from 0 to 1.0 V (SCE) in a 0.2 mM $Ru(CN)_6^{4-}$ and 0.1 M $LiClO_4$ solution. The thick lines are the experimental results and the thinner lines are the modeled results using $D_{CT} = 0$, $\Gamma = 2.8 \times 10^{-9}$ mol cm^{-2}, $k = 1$ cm s^{-1}.

To determine D_{CT} for lateral charge propagation, the full triple potential step method was employed. Figure 5 shows simulated results for the effect of D_{CT} on the transient for step 3, compared to the characteristics for step 1, with a waiting time of 30 min (for step 2) between the two steps. The results are shown for real parameter values, comparable to those encountered for this system: $k = 1$ cm s^{-1}, $d = 8.5$ μm ($a = 12.5$ μm), $\Gamma = 3.5 \times 10^{-9}$ mol cm^{-2}, $c^* = 0.2$ mM, $D = (7.46 \pm 0.03) \times 10^{-6}$ cm^2 s^{-1}; D_{CT} was varied over 2 orders of magnitude from 10^{-11} to

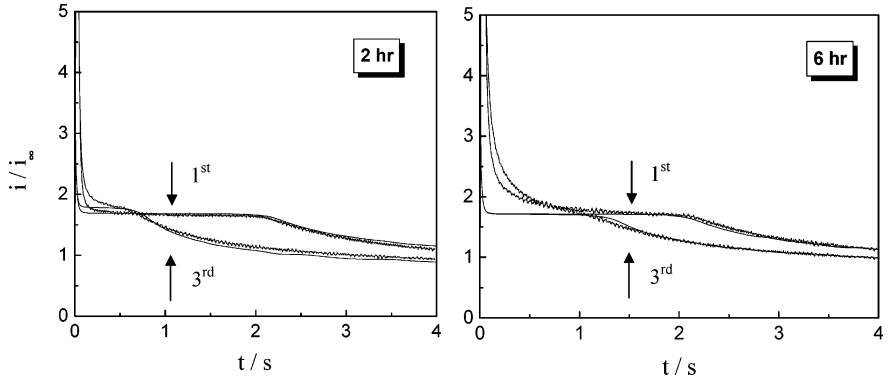

Figure 8. Current−time transients (for the first and third steps) to show the effect of waiting time (see box in each plot) on the recovery of charge carriers in a [Os(bpy)$_2$(PVP)$_{10}$Cl]Cl film. The thick lines are the experimental results, and the thin lines are the results of simulations using a value of $D_{CT} = 1.3 \times 10^{-10}$ cm^2 s^{-1}. For the waiting period of 2 h, $d = 8.8$ μm and for the waiting period of 6 h, $d = 9.7$ μm. For both cases, $\Gamma = 2.8 \times 10^{-9}$ mol cm^{-2} and $k = 1$ cm s^{-1} were used for the simulations.

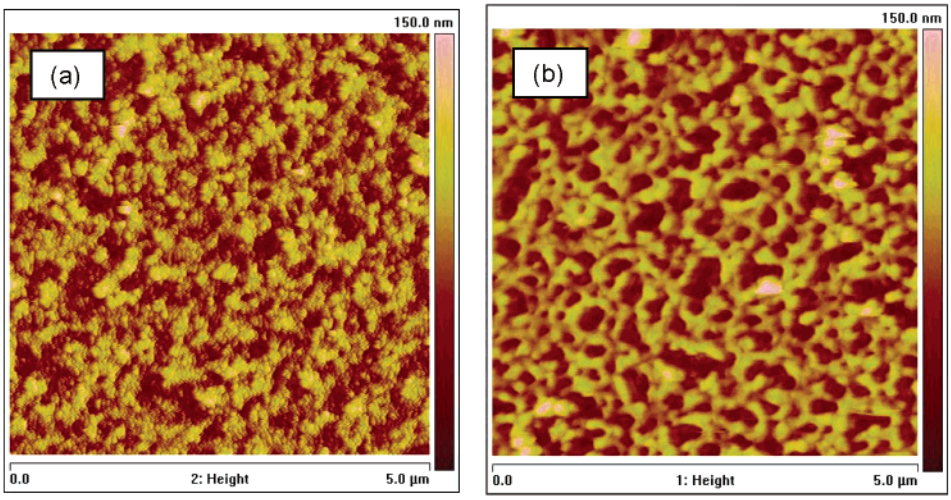

Figure 9. Tapping mode AFM topography images (5 μm × 5 μm) for (a) [Os(bpy)$_2$(PVP)$_5$Cl]Cl and (b) [Os(bpy)$_2$(PVP)$_{10}$Cl]Cl spin cast films.

10^{-9} cm^2 s^{-1}. It can be seen quite clearly that the recovery is highly dependent on D_{CT}: the larger the D_{CT} value, the greater the recovery of Os^{II} centers in step 2 and the greater tendency of the transient for step 3 toward that obtained in step 1. This figure also shows that the time at which the current decays between the positive feedback value and the hindered diffusion value is highly diagnostic of D_{CT}.

To determine D_{CT} experimentally, the optimum approach is to measure current−time transients for steps 1 and 3, while varying the length of the recovery period. Figure 6 shows typical experimental results for steps 1 and 3, for recovery times of 10, 20, 40, and 70 min. In these measurements, the length of the step 1 transient was shortened to 4 s (compared to the data in Figure 4a) to ensure recovery of the film on a reasonable time scale. The initial tip−sample distance was kept constant for each experiment at 8.5 μm, confirmed by simulating the tip current response with the parameters defined above. It can be seen quite clearly that the extent to which the feedback current flows in step 3 depends on the waiting period: the larger the waiting period, the greater the recovery toward the transient recorded in step 1. The data in Figure 6 were modeled for steps 1 and 3, using the parameters defined, yielding a value of (1.9 ± 0.2) × 10^{-9} cm^2 s^{-1} for D_{CT}. It can be seen in Figure 6 that the transients recorded for step 3 give a feedback current that increases slightly, with waiting time, compared to step 1. The origin of this effect is most likely slight piezo drift in the direction normal to the interface over these long waiting times. For the 10 and 20 min waiting times, the tip−sample distance was 7.5 μm, whereas for the 40 and 70 min waiting times a tip−sample distance of 7 μm was most appropriate when modeling these transients.

Under conditions where there is no physical diffusion of redox centers within the film and charge transport is due entirely to electron hopping, D_{CT} can be related to the electron self-exchange rate constant k_{ex} in the metallopolymer by the following[27]

$$D_{CT} = \lambda k_{ex} \delta^2 c_{film} \qquad (28)$$

where c_{film} is the concentration of charge carriers (surface coverage is taken as 3.5×10^{-9} mol cm^{-2} and the thickness as 90 nm), δ is the intersite separation between redox centers (1.25 nm as measured by Vos[4]), and λ depends on the dimensionality of the system. Although charge transport is lateral, the thickness of the film dictates that charge propagation is three-dimensional, for which $\lambda = 1/6$. For $D_{CT} = 1.9 \times 10^{-9}$ cm^2 s^{-1}, a value $k_{ex} = 1.9 \times 10^9$ mol^{-1} cm^3 s^{-1} results, which is in close agreement with the value obtained by Murray and co-workers[56] for a similar type of osmium metallopolymer.

Experiments using the same protocol were also carried out on [Os(bpy)$_2$(PVP)$_{10}$Cl]Cl films, in which the redox center concentration was lower than for the case discussed above. For this material, diffusion-controlled electron-transfer kinetics between the solution mediator and the redox centers was also observed ($k \geq 1$ cm s^{-1}) with again a strong distance effect for step 1, as illustrated in Figure 7. To model step 1 in this case,

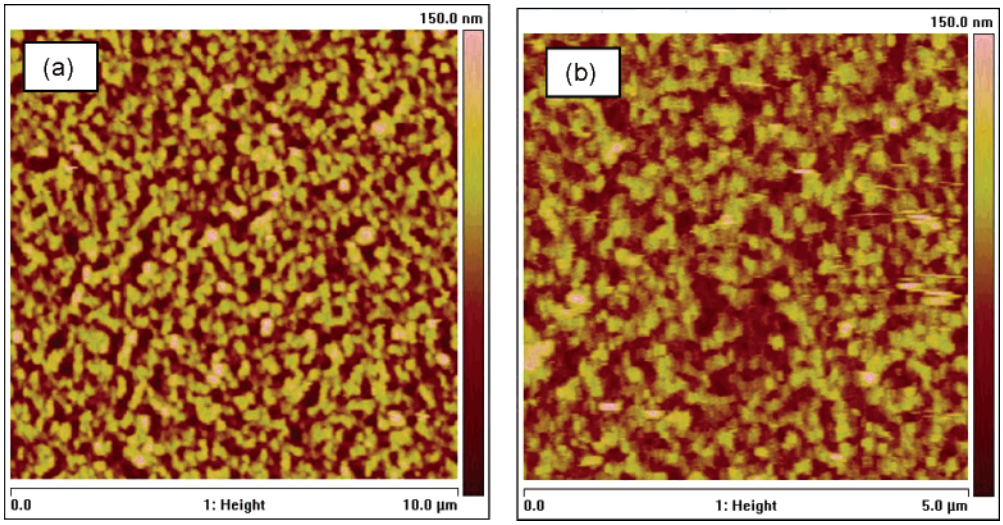

Figure 10. Contact mode AFM topography images of $[Os(bpy)_2(PVP)_5Cl]Cl$ in 0.1 M $LiClO_4$ solution at scan sizes of (a) (10 μm × 10 μm) and (b) (5 μm × 5 μm).

an Os redox center concentration of 2.8×10^{-9} mol cm^{-2} gave the best fit, which was again close to the value deduced from CV measurements (not shown). This value for the effective surface coverage of Os^{II} moieties is only slightly less than measured for $Os(bpy)_2(PVP)_5Cl]Cl$ because, as discussed below, there is a difference in the quality of the two films, with the $[Os(bpy)_2(PVP)_{10}Cl]Cl$ film showing a rougher surface and greater thickness of 100 ± 25 nm.

Figure 8 illustrates the response recorded for step 3 after waiting times of 2 and 6 h. The tip−sample distance for step 1 was 8.8 μm for the 2 h experiment and 9.7 μm for the 6 h experiment. To detect any recovery in the film, waiting times employed for step 2 were of the order of hours as compared to tens of minutes for the polymer of higher loading. Comparing the data in Figure 8 with that Figure 6, it can be seen that even after 6 h, recovery has occurred to a lesser extent than for the $[Os(bpy)_2(PVP)_5Cl]Cl$ film after 70 min. By fitting the transients in Figure 8 to the model outlined earlier, a value of $(1.3 \pm 0.5) \times 10^{-10}$ cm^2 s^{-1} for D_{CT} gave the best fit. This is an order of magnitude lower than that obtained for the $[Os(bpy)_2(PVP)_5Cl]$-Cl film. The lower value of D_{CT} for $[Os(bpy)_2(PVP)_{10}Cl]Cl$ is expected, given the greater intersite separation between redox centers, which was calculated to be 2.5 nm by Vos.[4] We have not estimated k_{ex} from eq 28 for this case because of heterogeneities in film structure highlighted below. However, the trend seen is clearly consistent with electron hopping as the limiting process in these measurements in contrast to earlier CV measurements where such effects were not apparent due to limiting ion transfer at the film/electrolyte interface.[4]

AFM Measurements. Tapping mode AFM images in air (Figure 9) indicate that these films have a fairly open, porous structure, although the $[Os(bpy)_2(PVP)_5Cl]Cl$ films appear to be more compact and homogeneous than the $[Os(bpy)_2$-$(PVP)_{10}Cl]Cl$ films. This may also be a significant factor in the larger values obtained for D_{CT} for $[Os(bpy)_2(PVP)_5Cl]Cl$ compared to $[Os(bpy)_2(PVP)_{10}Cl]Cl$. Contact mode AFM studies of $[Os(bpy)_2(PVP)_5Cl]Cl$ films under 0.1 M aqueous $LiClO_4$ solution show that the structure is maintained, as illustrated by the images in Figure 10.

Conclusions

We have shown that the SECM triple potential step technique is a viable approach for measuring the coefficient for lateral electron hopping (D_{CT}) in thin redox polymer films, and is capable of measuring values as low as 10^{-10} cm^2 s^{-1}. An advantage of the SECM approach is that it is entirely homogeneous and there are no complications from heterogeneous charge transfer from a metal electrode to the metallopolymer film, as required for conventional electrochemical techniques. Moreover, in the SECM technique, electron transfer and ion transfer occur at the same side of the film, and the perturbation in the redox state of the film occurs on relatively small length scales. This means that electron hopping is likely to be the limiting process measured.

For $[Os(bpy)_2(PVP)_5Cl]Cl$, D_{CT} was higher by an order of magnitude than for $[Os(bpy)_2(PVP)_{10}Cl]Cl$. Undoubtedly, the greater separation between redox sites in $[Os(bpy)_2(PVP)_{10}Cl]$-Cl was likely to be an important factor in the smaller value of D_{CT}, but a clear difference in film structure was also expected to have a contributory effect, with the more compact nature of the $[Os(bpy)_2(PVP)_5Cl]Cl$ films leading to a higher D_{CT} value.

Acknowledgment. We thank the EU Human Potential Program SUSANA (Supramolecular Self-Assembly of Interfacial Nanostructures), contract HPRN-CT-2002-00185, for funding. J.C. also thanks the financial support from CICYT (Ministry of Science and Technology of Spain) and FEDER (European Funds for Regional Development) under project No. MAT2002-00646.

References and Notes

(1) Anson, F. C.; Savéant, J.-M.; Shigehara, K. *J. Electroanal. Chem.* **1988**, *145*, 423.
(2) Feldman, B. J.; Ewing, A.; Murray, R. W. *J. Electroanal. Chem.* **1985**, *194*, 63.
(3) Forster, R. J.; Vos, J. G. *Electrochim. Acta* **1992**, *37*, 159.
(4) Forster, R. J.; Vos, J. G. *Langmuir* **1994**, *10*, 4330.
(5) Xie, Y.; Anson, F. C. *J. Electroanal. Chem.* **1995**, *384*, 145.
(6) Doherty, A. P.; Vos, J. G. *Anal. Chim. Acta* **1997**, *344*, 159.
(7) Pickup, P. G.; Kuo, K. N.; Murray, R. W. *J. Electrochem. Soc.* **1983**, *130*, 2205.
(8) Wilson, R. W.; Cubitt, R.; Glidle, A.; Hillman, A. R.; Saville, P. M.; Vos, J. G. *Electrochim. Acta* **1999**, *44*, 3533.
(9) Hogan, C. F.; Forster, R. J. *Anal. Chim. Acta* **1999**, *396*, 13.
(10) Ju, H.; Gong, Y.; Zhu, H. *Anal. Sci.* **2001**, *17*, 59.
(11) Forster, R. J.; Figgemeir, E.; Lees, A. C.; Hjelm, J.; Vos, J. G. *Langmuir* **2000**, *16*, 7867.
(12) Murray, R. W. *Molecular Design of Electrode Surfaces, Techniques of Chemistry*; Wiley-Interscience: Toronto, 1992; Vol. XXII.

(13) Schmel, R. H.; Murray, R. W. *J. Electroanal. Chem*. **1983**, *152*, 97.
(14) Jernigan, J. C.; Murray, R. W. *J. Am. Chem. Soc*. **1987**, *109*, 1738.
(15) Sosnoff, C. S.; Sullivan, M.; Murray, R. W. *J. Phys. Chem*. **1994**, *98*, 13643.
(16) Buttry, D. A.; Anson, F. C. *J. Electroanal. Chem*. **1981**, *130*, 333.
(17) Buttry, D. A.; Anson, F. C. *J. Am. Chem. Soc*. **1983**, *105*, 685.
(18) Anson, F. C.; Blauch, D. N.; Savéant, J.-M.; Shu, C.-F. *J. Am. Chem. Soc*. **1991**, *113*, 1922.
(19) Sabatani, R.; Anson, F. C. *J. Phys. Chem*. **1993**, *97*, 10158.
(20) Andrieux, C. P.; Dumas-Bouchiat, J. M.; Savéant, J. M. *J. Electroanal. Chem*. **1980**, *114*, 159.
(21) Andrieux, C. P.; Savéant, J. M. *J. Electroanal. Chem*. **1980**, *111*, 377.
(22) Savéant, J. M. *J. Electroanal. Chem*. **1987**, *238*, 1.
(23) Buck, R. P. *J. Electroanal. Chem*. **1988**, *243*, 279.
(24) Buck, R. P. *J. Phys. Chem*. **1988**, *92*, 4196.
(25) Buck, R. P.; Mădăraş, M. B. *J. Electroanal. Chem*. **1993**, *362*, 33.
(26) Kaneko, M. *Prog. Polm. Sci*. **2001**, *26*, 1101.
(27) Lyons, M. E G. In *Fundamentals*; Electroactive Polymer Chemistry, Part 1; Lyons, M. E. G., Ed.; Plenum Press: New York, 1994; Chapter 1, pp 1−226.
(28) Musiani, M. *Electrochim. Acta* **1990**, *35*, 1665.
(29) Larsson, H.; Sharp, M. *J. Electroanal. Chem.* **1995**, *381*, 133.
(30) Aoki, A.; Miyashita, T. *Colloids Surf. A: Physiochem. Eng. Aspects* **2002**, *198*−*200*, 671.
(31) Chidsey, C. E. D. *Science* **1986**, *231*, 25.
(32) Dalton, E. F.; Surridge, N. A.; Jernigan, J. C.; Wilbourn, K. O.; Facci, J. S.; Murray, R. W. *Chem. Phys.* **1990**, *141*, 143.
(33) Forster, R. J.; Keyes, T. E.; Majda, M. *J. Phys. Chem. B* **2000**, *104*, 4425.
(34) Wittek, M.; Moller, G.; Johnson, M. J.; Majda, M. *Anal. Chem.* **2001**, *73*, 870.
(35) Feldman, B. J.; Murray, R. W. *Anal. Chem*. **1986**, *58*, 2844.
(36) Feldman, B. J.; Feldberg, S. W.; Murray, R. W. *J. Phys. Chem*. **1987**, *91*, 6558.
(37) Forster, R. J.; Keyes, T. E.; Bond, A. M. *J. Phys. Chem. B* **2000**, *104*, 6389.
(38) Slevin, C. J.; Unwin, P. R. *J. Am. Chem. Soc*. **2000**, *122*, 2597.
(39) Zhang, J.; Unwin, P. R. *J. Am. Chem. Soc*. **2002**, *124*, 2379.
(40) Zhang, J.; Unwin, P. R. *Phys. Chem. Chem. Phys*. **2002**, *4*, 3814.
(41) Mandler, D.; Unwin, P. R. *J. Phys. Chem. B* **2003**, *107*, 407.
(42) Zhang, J.; Barker, A. L.; Mandler, D.; Unwin, P. R. *J. Am. Chem. Soc*. **2003**, *125*, 9312.
(43) Zhang, J.; Slevin, C. J.; Morton, C.; Scott, P.; Walton, D. J.; Unwin, P. R. *J. Phys. Chem. B* **2001**, *105*, 11120.
(44) Quinn, B. M.; Prieto, I.; Haram, S. K.; Bard, A. J. *J. Phys. Chem. B* **2001**, *105*, 7474.
(45) Liljeroth, L.; Quinn, B. M.; Ruiz, V.; Konturri, K. *Chem. Commun.* **2003**, 1570.
(46) (a) Wolf, D. E. In *Fluorescence Microscopy of Living Cells in Culture*; Taylor, D. L., Wang, Y. L., Eds.; Academic Press: San Diego, 1989; Part B, Chapter 10, p 271. (b) Elson, E. L.; Qian, H. In *Fluorescence Microscopy of Living Cells in Culture*; Taylor, D. L., Wang, Y. L., Eds.; Academic Press: San Diego, 1989; Part B, Chapter 11, p 307.
(47) Auch, M.; Ficher, B.; Möhwald, H. *Colloid Surf. A* **2000**, *164*, 39.
(48) Mullineaux, C. W.; Tobin, M. J.; Jones, G. R. *Nature* **1997**, *390*, 421.
(49) Axelrod, D.; Koppel, D. E.; Schlessinger, J.; Elson, E.; Webb, W. W. *Biophys. J.* **1976**, *16*, 1055.
(50) Unwin, P. R.; Bard, A. J. *J. Phys. Chem.* **1991**, *95*, 7814.
(51) Unwin, P. R.; Bard, A. J. *J. Phys. Chem.* **1992**, *96*, 5035.
(52) Newman, J. *J. Electrochem. Soc.* **1966**, *113*, 501.
(53) Saito, Y. *Rev. Polarogr. Jpn.* **1968**, *15*, 177−187.
(54) Forster, R. J.; Vos, J. G. *Macromolecules* **1990**, *23*, 4372.
(55) Kelly, D. M.; Vos, J. G. *J. Electroanal. Chem*. **1996**, *41*, 1825.
(56) Dalton, E. F.; Surridge, N. A.; Jernigan, J. C.; Wilbourn, K. O.; Facci, J. S.; Murray, R. W. *Chem. Phys.* **1990**, *141*, 143.